energy is $N(0) = 1.14$ eV^{-1} per copper atom. For Y$_1$Ba$_2$Cu$_3$O$_7$ the band arising from the chains would be half full if all holes were in this band. This would lead to $N(0) = 0.21$ eV^{-1} per chain copper. These results are used in the accompanying report (12) to derive the T_c for superconductivity in cuprates.
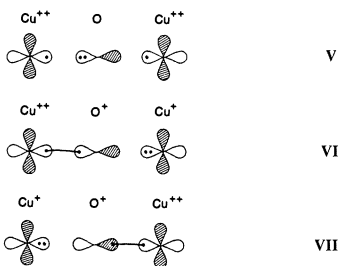
The Hubbard model. As pointed out above, standard HF methods lead to a very bad description of systems such as these Cu^{II} systems having weakly overlapping orbitals. The result is a strong mixture of the singly occupied $d\sigma$ orbitals ($d_{y^2-z^2}$ pointing from Cu to O) with oxygen $p\sigma$ orbitals, leading to a partially filled band of mixed copper $d\sigma$ and oxygen $p\sigma$ character. With GVB, the electron correlation effects lead to singly occupied $d_{y^2-z^2}$ orbitals on each copper. In terms of band concepts this GVB description corresponds to half occupation of every orbital of the band constructed from $d_{y^2-z^2}$ on each center, whereas HF would start with half occupation of the band. The Hubbard approximation (14) to UHF builds in a similar improvement upon standard HF band theory by introducing a repulsive one-center term to split the HF band into up-spin and down-spin bands on separate sublattices (leading to spin waves). The GVB approach treats the electron correlation problem rigorously, leading to pure spin states. However, this leads to the complication that the band states must be calculated in terms of N-body wavefunctions (as presented above) rather than the usual one-particle orbitals.

Several standard one-electron band calculations (based on local density functionals) have been reported (15) on La$_2$Cu$_1$O$_4$. These band calculations suggest an overall population of d^9 on each copper, in agreement with the GVB results but, as expected, they all involve strong mixing of copper $d\sigma$ and oxygen $p\sigma$ character, leading to a partially occupied band of σ character. A properly parameterized Hubbard Hamiltonian might mimic the GVB results (with the copper $d\sigma$ orbitals forming a narrow band and a highest band that is oxygen $p\pi$–like).

REFERENCES AND NOTES

1. J. G. Bednorz and K. A. Müller, Z. Phys. B 64, 189 (1986); J. M. Tarascon, L. H. Greene, W. R. McKinnon, G. W. Hull, T. H. Geballe, Science 235, 1373 (1987).
2. M. K. Wu, et al., Phys. Rev. Lett. 58, 908 (1987).
3. W. J. Hunt, P. J. Hay, W. A. Goddard III, J. Chem. Phys. 57, 738 (1972); W. A. Goddard III and T. C. McGill, J. Vac. Sci. Technol. 16, 1308 (1979).
4. The geometries of these clusters are based on neutron diffraction data (5). The Dunning (9s5p/3s2p) double zeta contraction (6) of the Huzinaga Gaussian basis set is used for the oxygen atoms. The Los Alamos core effective potential (7) is used to replace the 18 core electrons of the copper atom. This leads to a (3s,2p,2d) Gaussian basis for the 11 valence electrons of the copper atom.
5. P. Day et al., J. Phys. C 20, L429 (1987); W. I. F. David et al., Nature (London) 327, 310 (1987).
6. T. H. Dunning, Jr., and P. J. Hay, in Modern Theoretical Chemistry (Plenum, New York, 1977), vol. 3, p. 1.
7. P. J. Hay and W. R. Wadt, J. Chem. Phys. 82, 270 (1985).
8. N. D. Mermin and H. Wagner, Phys. Rev. Lett. 17, 1133 (1966).
9. D. Vaknin et al., ibid. 58, 2802 (1987).
10. J. B. Torrance, Y. Tokura, A. Nazzal, S. S. P. Parkin, in preparation; Y. Tokura, J. B. Torrance, A. I. Nazzal, T. C. Huang, C. Ortiz, in preparation.
11. Superexchange involves mixing of charge transfer states (structures VI and VII) into the dominant wavefunction (top structure V diagram). This charge transfer is much less favorable if the oxygen is made more positive.

12. G. Chen and W. A. Goddard III, Science 239, 899 (1988).
13. A. F. Voter and W. A. Goddard III, J. Am. Chem. Soc. 108, 2830 (1986). The matrix elements as defined in Eq. 13 would depend on cluster size. We use instead

$$\bar{H}_{ij} = E^{N-1} S_{ij}^{N-1} - H_{ij}^{N-1} \qquad (20)$$

where E^{N-1} is the energy of the cluster with one hole, and H_{ij}^{N-1} and S_{ij}^{N-1} are for systems with the hole localized on sites i and j, respectively. The sign chosen in $\bar{H}_{ij}$ is so that $E_k = -IP_k$, where IP_k is the ionization potential out of Bloch state k, leading to band diagrams analogous to one-electron band diagrams.
14. J. Hubbard, Proc. R. Soc. London Ser. A. 281, 401 (1964).
15. L. F. Mattheiss, Phys. Rev. Lett. 58, 1028 (1987); K. Takegahara, H. Harima, A. Yanase, Jpn. J. Appl. Phys. 26, L352 (1987); T. Oguchi, ibid., p. L417.
16. We thank the Office of Naval Research and the donors of the Petroleum Research Fund (administered by the American Chemical Society) for partial support of this research. We thank C. M. Kao and G. Chen for assistance and useful discussions. The GVB and R-GVB calculations were carried out on the Alliant FX8/8 and DEC VAX 8650 computers in the Caltech Materials Simulation Facility [funded by the National Science Foundation–Materials Research Groups (grant DMR-84-21119); the Office of Naval Research/Defense Advanced Research Projects Agency (contract N00014-86-K-0735); the Department of Energy–Energy Conversion and Utilization Technology (JPL code 49-242-E0403-0-3550), the National Science Foundation–Chemistry (grant CHE-8318041), and the Office of Naval Research (contract N00014-84-K-0637)].

7 December 1987; accepted 20 January 1988

The Magnon Pairing Mechanism of Superconductivity in Cuprate Ceramics

GUANHUA CHEN AND WILLIAM A. GODDARD III

The magnon pairing mechanism is derived to explain the high-temperature superconductivity of both the La$_{2-x}$Sr$_x$Cu$_1$O$_4$ and Y$_1$Ba$_2$Cu$_3$O$_7$ systems. Critical features include (i) a one- or two-dimensional lattice of linear Cu-O-Cu bonds that contribute to large antiferromagnetic (superexchange) coupling of the Cu^{II} (d^9) orbitals; (ii) holes in the oxygen $p\pi$ bands [rather than Cu^{III} (d^8)] leading to high mobility hole conduction; and (iii) strong ferromagnetic coupling between oxygen $p\pi$ holes and adjacent Cu^{II} (d^9) electrons. The ferromagnetic coupling of the conduction electrons with copper d spins induces the attractive interaction responsible for the superconductivity, leading to triplet-coupled pairs called "tripgems." The disordered Heisenberg lattice of antiferromagnetically coupled copper d spins serves a role analogous to the phonons in a conventional system. This leads to a maximum transition temperature of about 200 K. For La$_{1.85}$Sr$_{0.15}$Cu$_1$O$_4$, the energy gap is in excellent agreement with experiment. For Y$_1$Ba$_2$Cu$_3$O$_7$, we find that both the CuO sheets and the CuO chains can contribute to the supercurrent.

T HE EXCITING DISCOVERIES FIRST of the 2-1-4 class of high-temperature superconductors (1) (best is, La$_{2-x}$Sr$_x$Cu$_1$O$_4$ with transition temperature $T_c = 40$ K) and then of the much higher temperature 1-2-3 system (2) (Y$_1$Ba$_2$Cu$_3$O$_7$ with $T_c = 93$ K) have led to a frenzied chase after even higher temperature superconductors and more easily processed materials. Simultaneously, the theoretical community

Arthur Amos Noyes Laboratory of Chemical Physics, California Institute of Technology, Pasadena, CA 91125.

has struggled with how to understand the origin of the superconductivity in these conducting ceramics. The need for such a theory is reinforced by the lack of any substantial increase in T_c, despite an enormous effort by materials scientists around the world (3). The problem has been the lack of a theoretical framework within which one could reason about the likely effects of various changes in composition or structure. We propose here such a model.

Recent calculations (4) indicate that the La$_{2-x}$Sr$_x$Cu$_1$O$_4$ and Y$_1$Ba$_2$Cu$_3$O$_7$ classes of

superconductor ceramics (1, 2) have the following features:

1) A network of Cu^{II} (d^9) sites with the singly occupied d orbital localized in the plane of four short Cu-O bonds (~1.9 Å).

2) The spins of adjacent d orbitals are coupled antiferromagnetically (by means of the intervening oxygen) with $J_{dd} = -205$ K for sheets and $J_{dd} = -244$ K for chains, where J_{dd} is the exchange integral.

3) Oxidation of the system beyond cupric (Cu^{II}) leads not to Cu^{III} but rather to holes localized in the $p\pi$ orbitals of oxygens.

$$O-Cu^{II}-O-Cu^{II}-O\rightarrow$$
$$O-Cu^{II}-O^+-Cu^{II}-O \qquad (1)$$
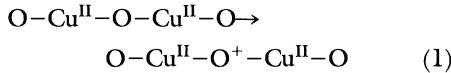
These $p\pi$ orbitals are localized in the plane involving the short Cu-O bonds to the adjacent copper.

4) The magnetic coupling of the singly occupied oxygen orbital with the adjacent copper electrons is ferromagnetic (J_{OCu} = 383 K for sheets and 405 K for chains). This leads to ferromagnetic coupling of the spins in the two copper atoms, despite the antiferromagnetic J_{dd}.

5) The migration of a hole from one site to another leads to energy bands with a width of 1.6 eV for chains and 1.4 eV for the upper band in sheets.

In this report we show that these features lead to superconductivity, with the attractive interaction between the conduction electrons arising from magnetic interactions [rather than the electron-phonon interactions of Bardeen-Cooper-Schrieffer (BCS) theory (5)].

To examine these interactions, we use the Hamiltonian,

$$H_{eff} = H_p + H_d + H_{pd} \qquad (2)$$

where

$$H_p = \sum_{k\sigma} \epsilon(k) A_{k\sigma}^\dagger A_{k\sigma} \qquad (3)$$

is the Hamiltonian for holes on oxygens (in the average field of d electrons on Cu^{II}),

$$H_d = -\sum_{(d_i d_j)} 2 J_{dd} \mathbf{S}_{di} \cdot \mathbf{S}_{dj} \qquad (4)$$

is the Hamiltonian for interaction of d electrons on adjacent Cu^{II} (ignoring p holes on oxygens), and

$$H_{pd} = -\sum_{(p_i d_j)} 2 J_{pd} \mathbf{S}_{pi} \cdot \mathbf{S}_{dj} \qquad (5)$$

is the interaction between oxygen $2p\pi$ holes and adjacent copper d electrons. Here we have taken (i) $A_{k\sigma}^\dagger$ and $A_{k\sigma}$ as the creation and annihilation operators for holes on oxygens, respectively; (ii) $\mathbf{S}_{di}$ as the spin operator for a d electron on site i; (iii) $\mathbf{S}_{pj}$ as the spin operator for an oxygen $2p\pi$ hole on site

j; (iv) J_{dd} as the exchange energy (negative) between adjacent copper d electrons; (v) J_{pd} as the exchange energy (positive) between adjacent oxygen p and copper d electrons; and (vi) $\epsilon(k)$ is the band energy for the oxygen $2p\pi$ hole state with wave vector $\mathbf{k}$.

At $T = 0$ K, the ground state of H_d is a Heisenberg singlet state (6). This leads to a vast number of spin configurations $N_{Cu}!/[(N_{Cu}/2)!]^2$, where N_{Cu} = number of Cu sites, all of which have significant contributions. Although there is a preference for adjacent copper d spins to have singlet pairing, even at 0 K most spin configurations have some triplet pairing. Writing

$$\tau = -2\langle \mathbf{S}_{di} \cdot \mathbf{S}_{dj} \rangle \qquad (6)$$

as the average (negative) spin polarization for adjacent copper d spins, the total magnon energy (from H_d) is

$$E_d = -\nu \tau N_{Cu} |J_{dd}| \qquad (7)$$

where ν is the dimensionality ($\nu = 1$ or 2).

The lowest order coupling process arises from the diagrams of Fig. 1, where only processes with the same initial and final states of the magnon background are examined. Each vertex leads to a factor of the form $2 J_{pd} P_Q$, where

$$P_Q \equiv \left[\cos\left(Q_x \frac{a_x}{2}\right) + (\nu - 1) \cos\left(Q_y \frac{a_y}{2}\right) \right] \qquad (8)$$

$\mathbf{Q} = \mathbf{k}_3 - \mathbf{k}_1$ is the scattering vector, ν is the number of dimensions, and ($a_i/2$) is the Cu-O separation in the x or y direction (for $\nu = 1$, only the x term is present). The self-energy for the copper d spin flip at the first vertex is

$$\epsilon_{sf} = 4\nu\tau |J_{dd}| \qquad (9)$$

where the copper d spin sees 2ν neighbors. To second order the scattering matrix element is

$$V_{k''\sigma'',k'''\sigma''',k\sigma,k'\sigma'} = -\frac{i}{2\pi} \left\langle k''\sigma'',k'''\sigma'''; \Psi_{back} \right.$$

$$\left| \left(\frac{i}{\hbar}\right)^2 \int dt_1 \int dt_2 T[H_{pd}(t_1) H_{pd}(t_2)] \right|$$

$$\left. k\sigma, k'\sigma'; \Psi_{back} \right\rangle \qquad (10)$$

where Ψ_{back} is the background of copper d magnetic states and T is the time-ordering operator. Thus,

$$V_{k''\sigma'',k'''\sigma''',k\sigma,k'\sigma'} = -\frac{4 P_Q^2 J_{pd}^2}{N_{Cu} \epsilon_{sf}} \equiv -W_Q \qquad (11)$$

where $\sigma \neq \sigma'$, $Q = k'' - k$, and W_Q is positive. Combining each pair of momentum state $\mathbf{k}_a$, $\mathbf{k}_b$ into spin singlets,
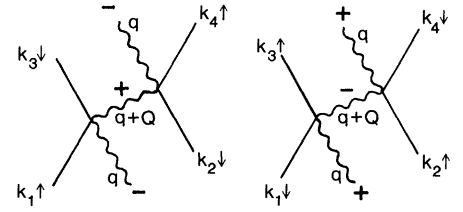

Fig. 1. Lowest order diagrams for coupling of conduction electrons (denoted by momenta $\mathbf{k}_i$ and spins ↑ and ↓) by means of copper d magnons (denoted as + or −).

$$(\mathbf{k}_a, \mathbf{k}_b)^S = \frac{1}{\sqrt{2}} (\mathbf{k}_a \mathbf{k}_b + \mathbf{k}_b \mathbf{k}_a) \chi_0 \qquad (12)$$

and spin triplets

$$(\mathbf{k}_a, \mathbf{k}_b)^T = \frac{1}{\sqrt{2}} (\mathbf{k}_a \mathbf{k}_b - \mathbf{k}_b \mathbf{k}_a) \chi_1 \qquad (13)$$

leads to

$$V_{(kc,kd)^T, (ka,kb)^T} = -W_{kc-ka} + W_{kd-ka} \qquad (14)$$

$$V_{(kc,kd)^S, (ka,kb)^S} = +W_{kc-ka} + W_{kd-ka} \qquad (15)$$

$$V_{(kckd)^S, (kakb)^T} = 0 \qquad (16)$$

$$V_{(kckd)^T, (kakb)^S} = 0 \qquad (17)$$

where $\chi_0 = (\alpha\beta - \beta\alpha)/\sqrt{2}$ and $\chi_1 = (\alpha\beta + \beta\alpha)/\sqrt{2}$ are singlet and triplet spin functions, respectively. Thus there is an attractive coupling for triplet states and a repulsive coupling for singlet states.

Considering the "tripgems" (triplet geminal pairs), $(\mathbf{k}, -\mathbf{k})^T$, the attractive coupling between tripgems,

$$V_{kk'} \equiv V_{(k',-k')^T,(k,-k)^T} = -W_{k'-k} + W_{-k'-k} \qquad (18)$$

leads to an energy gap. The differences between the magnon pairing theory and BCS theory are that (i) the medium providing the coupling involves the copper d magnons rather than lattice phonons; (ii) the coupling of conduction electrons to the medium is by localized magnetic coupling rather than by electron-phonon coupling; and (iii) the ground state involves triplet pairs $(\mathbf{k}, -\mathbf{k})^T$, tripgems, in place of the singlet Cooper pairs of BCS theory.

Since $V_{kk'} = -V_{k,-k'}$, the first term in the Fourier expansion of $V_{kk'}$ is $V_{kk'} = V_k^{(1)}$ cos $\theta_{kk'}$, where $\theta_{kk'}$ is the angle between $\mathbf{k}$ and $\mathbf{k}'$. Defining the average value of $V_k^{(1)}$ as $\overline{V}^{(1)}$ leads to

$$\overline{V}^{(1)} = -\frac{1}{2} W_0 \equiv -\frac{\overline{W}}{N_{Cu}} \qquad (19)$$

where

$$\overline{W} = \frac{1}{2} \frac{4\nu^2 J_{pd}^2}{4\nu\tau |J_{dd}|} = \frac{\nu J_{pd}^2}{2\tau |J_{dd}|} \qquad (20)$$

The result is an energy gap of (8)

$$\frac{2\Delta}{k_B T_c} = \frac{2\left[\sinh\left(\frac{1}{\overline{N}_0 \overline{W}}\right)\right]^{-1}}{1.13 \exp[-(1/\overline{N}_0 \overline{W})]} \quad (21)$$

and a critical temperature for superconductivity of (7)

$$T_c = 1.13 |J_{dd}| \exp\left(-\frac{1}{\overline{N}(0)\overline{W}}\right) \quad (22)$$

where $\hbar\omega_g \approx |J_{dd}|$ and $N(0) = \overline{N}_0 N_{Cu}$ is the electronic state density at the Fermi energy (for the oxygen $p\pi$ band).

To examine the consequences of Eq. 21, consider $La_{2-x}Sr_xCu_1O_4$, which exhibits $T_c = 40$ K for $x = 0.15$. With $J_{dd} = -204.8$ K and $J_{pd} = 383.0$ K from generalized valence bond (GVB) calculations (4) and $\overline{N}_0 = 1.14$ eV^{-1} from GVB energy band calculations (4) leads to $\overline{N}(0)\overline{W} = 0.0705/\tau$. Thus, $\tau = 0.05$ leads to $\overline{N}(0)\overline{W} = 1.41$, $2\Delta/k_B T_c = 4.67$, and $T_c = 0.56|J_{dd}| = 114$ K. With $\tau = 0.02$ one obtains $\overline{N}(0)\overline{W} = 3.52$, $(2\Delta/k_B T_c) = 8.1$, and $T_c = 0.85 |J_{dd}| = 174$ K. This energy gap is in excellent agreement with experiment, in which $(2\Delta/k_B T_c)_{exp} = 4.5$ (9) and 7 ± 2 (10). The predicted transition temperature of 114 K is larger than observed (40 K); however, Eq. 22 is much more sensitive to various approximations than Eq. 21.

The predictions are sensitive to the net magnon polarization τ, which is the only parameter not determined here from first principles. A perfectly ordered antiferromagnetic Ising lattice has $\tau = 0.5$, which would lead to $\overline{N}(0)\overline{W} = 0.141$, and hence $T_c = 0.0009 |J_{dd}| = 0.2$ K. The optimum magnon polarization for superconductivity is $\tau = 0$, which would lead to $\overline{N}_0\overline{W} = \infty$ and hence $T_c \equiv |J_{dd}| = 205$ K (in the strong coupling limit for T_c). We expect a decrease in τ as the number of holes in the oxygen $p\pi$ band is increased (since the oxygen $p\pi$ holes tend to couple the copper d spins ferromagnetically) and τ should be decreased by the supercurrent. Above T_c, the experimental magnetic susceptibility could be combined with the theoretical J_{dd} to derive τ. The quantity τ could be derived by combining the experimental magnetic susceptibility above T_c with the theroretical J_{dd}. We are carrying out simulations with Eq. 2 to determine τ as a function of various parameters.

It is more difficult to estimate the T_c and gap for $Y_1Ba_2Cu_3O_7$ because of uncertainties concerning the relative number of holes in the oxygen $p\pi$ band of the chains and sheets and in the corresponding values of τ. This is exacerbated for $Y_1Ba_2Cu_3O_y$ with $y \ne 7$ due to uncertainties as to the location of the oxygen vacancies. The theory suggests that the supercurrent can be carried either

by the Cu-O chains or by the Cu-O sheets (much as in $La_{2-x}Sr_xCuO_4$) or by both. With the ideal composition of $Y_1Ba_2Cu_3O_7$, there is one oxygen $p\pi$ hole per every three copper atoms. The GVB calculations (4) show that the favorable location for oxidation [beyond Cu(II)] is the chain oxygens. However, for $y = 7$, this would require half the oxygen $p\pi$ electrons to be removed from the Cu-O chain (11). The calculations suggest that some oxidation occurs in both the sheets and the chains. Superconductivity is observed in $Y_1Ba_2Cu_3O_7$ for y as low as 6.3 (12), but $T_c \sim 55$ K for $y = 6.3$ to 6.6 (12), whereas $T_c \sim 93$ K for $y = 6.8$ to 7.0 (12). It is likely that most of the oxygen atom vacancies required for $y < 7$ are along the Cu-O chains. For $y = 6.8$ to 7.0, we believe that the supercurrent is carried by both sheets and chains. Because there is weak ferromagnetic coupling ($J_{dd} = 11$ K) between the sheet copper and the chain copper (through the bridge oxygen, O_B), the τ for both sheets and chains should decrease (thereby increasing the T_c for sheets from the value in $La_{1.85}Su_{0.15}CuO_4$).

If the highest temperature superconductivity ($T_c = 93$ K) were solely the result of the chains and if all oxygen $p\pi$ holes were in the chain oxygen $p\pi$ band, the values of $J_{dd} = -244$ K and $J_{pd} = 405$ K from the GVB calculations (4) and $\overline{N}_0 = 0.21$ eV^{-1} per chain copper from GVB energy band calculations (4) lead to

$$\overline{N}_0\overline{W} = \frac{\overline{N}_0 J_{pd}^2}{2\tau |J_{dd}|} = \frac{0.00609}{\tau} \quad (23)$$

Thus, to obtain $\overline{N}_0\overline{W} = 1.41$ ($T_c = 114$ K) would require $\tau = 0.0043$, a factor of 10 smaller than assumed for $La_{1.85}Sr_{0.15}Cu_1O_4$. On the other hand, if the sheets were solely responsible, then assuming all parameters as in $La_{1.85}Sr_{0.15}Cu_1O_4$ but decreasing τ from 0.05 to 0.02 would increase the predicted T_c from 114 K to 174 K, an increase of about 60 K. As mentioned above, the ferromagnetic coupling between sheets and chain copper should tend to disrupt the antiferromagnetic coupling in both the chains and sheets, leading to smaller τ.

We suggest that the superconductivity for $y = 6.3$ to 6.6 may arise solely from sheets, leading to a T_c similar to that of $La_{2-x}Sr_x$-CuO_4. An exact prediction is difficult since the actual number of holes in the oxygen $p\pi$ bands of the sheets is unknown, as is the effective value of τ (it should be lower than $La_{1.85}Sr_{0.15}CuO_4$). For $y < 6.2$, these systems are not superconducting; we believe that this is due to a lack of oxygen $p\pi$ holes in the sheets.

Emery (13) has suggested an origin of the superconductivity in these systems that has

some resemblance to the magnon pairing mechanism. He constructed a Hubbard Hamiltonian model that would have partially occupied copper $d\sigma$ and oxygen $p\sigma$ bands and suggested that an attractive coupling by means of magnetic exchange with copper d spins might lead to a strong attractive coupling of the oxygen $p\sigma$ electrons. Although the detailed mechanism is quite different from our theory, the work of Emery showed insight into the fundamental physics. A major difference is that Emery assumed that a band of oxygen $p\sigma$ holes was relevant (as would be expected from the one-electron band calculations) rather than the oxygen $p\pi$ holes found from GVB calculations (4). This led Emery to postulate singlet pairing of such oxygen $p\sigma$ orbitals. An elaboration of the Emery suggestion was carried out by Hirsch (14). Here, strong coupling was assumed and the attractive coupling was visualized in terms of oxygen $p\sigma$ hole migration coupled with flipping of copper d spins followed by reflipping of these spins as the result of a second oxygen $p\sigma$ hole. Hirsch suggests that this might lead to a finite confinement of the two oxygen $p\sigma$ holes. The GVB calculations (4) show that such strongly coupled pairs are not stable (the residual Coulomb repulsion makes it unfavorable to localize oxygen p holes on nearby sites relative to the energy of two separated holes). Rather, we find the attractive coupling to arise in the weak coupling limit (analogous to BCS theory except that the interactions are magnetic in origin). This leads to the coupling of triplet pairs and p-wave coupling rather than the coupling of singlet pairs and s-wave coupling.

Anderson (15, 16) has suggested a model for La_2CuO_4 in which adjacent copper d^9 atoms are single spin-paired (valence bond) and in which there is additional oxidation out of some copper d^9 orbitals to yield singlet copper d^8. He proposed a resonating valence bond description of conduction in which the strongly coupled singlet pairs move about as bosons (15, 16) rather than as a normal simple hole conduction of an antiferromagnetic system. He suggested that this strong pairing model would explain the superconductivity of the cuprates and predicted a gapless superconductor (16) [experimentally, there is a gap (9, 10)]. This Anderson model is quite different from the magnon-pairing model (where we have holes in the oxygen $p\pi$ orbitals, a large gap, and attractive pairing involving triplet coupling).

Essential points in the superconductivity of these cuprates are as follows:

1) The fact that the Cu^{II} d electrons form a two-dimensional (or one-dimensional) Heisenberg lattice is crucial, leading to

large quantum spin fluctuations (6) at low temperatures. The ordering temperature for a one- or two-dimensional Heisenberg spin lattice is 0 K, whereas a three-dimensional system would condense into long-range order at about (17) $3J_{dd}$, leading to small spin fluctuations at low temperature.

2) The large superexchange of the linear Cu-O-Cu bonds leads to large negative J_{dd} and hence to high-frequency spin waves.

3) In the CuO sheets and chains, oxygen $p\pi$ holes on adjacent oxygens have large matrix elements leading to high mobility (allowing the holes to move freely).

4) The ferromagnetic pairing between the localized oxygen $p\pi$ hole and the adjacent copper d electron couples the conduction electrons to the copper d magnons, leading to the attractive pairing responsible for superconductivity.

5) For the 1-2-3 system, the one-dimensional Cu-O chains may play more than one important role. Perfect chains would indeed lead to superconductivity; however, the specific value of T_c depends sensitively upon the average magnon polarization, τ. The ferromagnetic coupling between chains and sheets may lead to a decreased τ that increases T_c for superconductivity in both the chains and sheets. For values of y (in $Y_1Ba_2Cu_3O_y$) around $y = 6.5$ (and for the tetragonal phase), the observed superconductivity may be due to sheets.

6) The equations for T_c and Δ, Eqs. 21 and 22, clearly indicate those quantities that should be maximized and minimized in order to develop higher temperature superconductors.

A qualitative view of the magnon-pairing model is as follows. A conduction electron (oxygen $p\pi$-like) tends to repolarize the nearby copper d spins into local ferromagnetic order. As this oxygen $p\pi$ electron moves along, it tends to leave behind a wake with ferromagnetically paired copper spins. As a second conduction electron is scattered, it finds it favorable to be scattered into the wake of the first electron since there is already ferromagnetic polarization of the copper spins. The net result is the attractive interaction responsible for superconductivity.

One puzzle in understanding these systems concerns why $La_{2-x}Sr_xCrO_4$ is not a superconductor beyond $x = 0.3$ and why other systems (such as $La_4BaCu_5O_{13}$ and $La_5SrCu_6O_{15}$) (18) with similar sheets and chains and a high level of oxidation are semiconductors. In our mechanism, this is easily explained in terms of subtle shifts in the net Madelung energy at each oxygen (because of changes in location and charge of cations) that shifts the relative oxidation potential of various oxygens. This arises

because the magnon-pairing model requires holes in the proper oxygen $p\pi$ orbital of the sheets and chains. Thus, Guo et al. (4) showed that changing x from 0 to 0.3 in $La_{2-x}SrCuO_4$ shifts the lowest ionization potential from the sheet oxygen to the apex oxygen (which does not contribute to superconductivity). This suggests that the above semiconducting cuprates might be made into superconductors by appropriate replacement of cations or changes in structure.

REFERENCES AND NOTES

1. J. G. Bednorz and K. A. Müller, Z. Phys. B 64, 189 (1986); J. M. Tarascon et al., Science 235, 1373 (1987).
2. M. K. Wu et al., Phys. Rev. Lett. 58, 908 (1987).
3. L. Garwin and P. Campbell, Nature (London) 330, 611 (1987).
4. Y. Guo et al., Science 239, 896 (1988).
5. J. Bardeen, L. N. Cooper, J. R. Schrieffer, Phys. Rev. 108, 1175 (1957).
6. N. D. Mermin and H. Wagner, Phys. Rev. Lett. 17, 1133 (1966).
7. P. W. Anderson, Basic Notions of Condensed Matter Physics (Benjamin/Cummings, Menlo Park, 1984).
8. A. L. Fetter and J. D. Walecka, Quantum Theory of Many-Particle Systems (McGraw-Hill, New York, 1971).
9. S. Pan, K. W. Ng, A. L. de Lozanne, J. M. Tarascon, L. H. Greene, Phys. Rev. B 35, 7220 (1987).
10. J. R. Kirtley et al., ibid., p. 7216.
11. Only oxygen $p\pi$ orbitals parallel to the plane of the chain are considered.
12. M. Tokumoto et al., Jpn. J. Appl. Phys. 26, L1565 (1987).
13. V. J. Emery, Phys. Rev. Lett. 58, 2794 (1987).
14. J. E. Hirsch, ibid. 59, 228 (1987).
15. P. W. Anderson, Science 235, 1196 (1987).
16. P. W. Anderson et al., Phys. Rev. Lett. 58, 2790 (1987).
17. J. S. Smart, Effective Field Theories of Magnetism, (Saunders, Philadelphia, 1966), p. 26.
18. J. B. Torrance, Y. Tokura, A. Nazzal, S. S. P. Parkin, in preparation; Y. Tokura, J. B. Torrance, A. I. Nazzal, T. C. Huang, C. Ortiz, in preparation.
19. We thank the Office of Naval Research for partial support of this research and thank Y. Guo and J.-M. Langlois for useful interactions. The GVB calculations on which this magnon-pairing theory is based were carried out on the Alliant FX8/8 and DEC VAX 8650 computers in the Caltech Materials Simulation Facility [funded by the National Science Foundation–Materials Research Groups (grant DMR-84-21119); the Office of Naval Research/Defense Advanced Research Projects Agency (contract N00014-86-K-0735); the Department of Energy–Energy Conversion and Utilization Technology (JPL code 49-242-E0403-0-3550), the National Science Foundation–Chemistry (grant CHE-8318041), and the Office of Naval Research (contract N00014-84-K-0637)].

7 December 1987; accepted 20 January 1988

Spectroscopic Evidence for Pressure-Induced Coordination Changes in Silicate Glasses and Melts

QUENTIN WILLIAMS AND RAYMOND JEANLOZ

Infrared spectra demonstrate that at pressures above 20 gigapascals and room temperature the regular tetrahedral coordination of oxygen around both silicon and aluminum ions is severely disrupted in SiO_2, $CaMgSi_2O_6$, and $CaAlSi_2O_8$ composition glasses. The spectra are consistent with gradual, pressure-induced increases in the coordination numbers of silicon and aluminum. A variety of coordination environments, from sixfold to fourfold, appears to be present at pressures as high as about 40 gigapascals. This apparent change in coordination is not quenchable at room temperature: on decompression, the glasses return to tetrahedral coordination. This continuous and reversible coordination change in amorphous silicates explains the lack of observation of coordination changes in silicate glasses quenched from high pressure, the shallow melting slopes observed for mantle silicates at high pressures, and the possible presence of neutrally buoyant magmas deep within the terrestrial planets.

THE PROPERTIES OF SILICATE MELTS, such as density, viscosity, and chemical diffusivity, control processes of differentiation by which the interiors of Earth and other terrestrial planets evolve over geological time. As melt properties are largely determined by the geometrical packing and coordinations of ions, there has been considerable interest in documenting how the structures of both melts and glasses change with pressure, or in the case of planets, with increasing depth.

At ambient conditions, silicate melts and glasses are structurally ordered in the sense

that they exhibit a well-defined nearest neighbor coordination of four oxygen ions around silicon and aluminum ions. Under pressure, however, it is expected that the coordination increases from fourfold (tetrahedral arrangement) to sixfold (octahedral arrangement), resulting in a drastic change in melt properties (1). This expectation is based on the coordination changes observed among crystalline silicates under pressure. That such a change occurs in melts and

Department of Geology and Geophysics, University of California, Berkeley, CA 94720.